Chapter 16
Light and Electron Microscopy

Heike Bunjes and Judith Kuntsche

Abstract Microscopic techniques have a long history in pharmaceutical formulation research and development. They are especially useful for the study of systems containing particles of different length scales (like powders, granules, or colloidal suspensions) but can also be employed for the study of compact solid forms like tablets or of semisolids. As they yield a visual impression of the object of study they provide a rather natural way to the comprehension of sample behavior. As with all analytical techniques, however, there may be limitations and pitfalls that should be known in order to employ the methods correctly. This chapter explains the basic features of the microscopic techniques traditionally employed in pharmaceutical research—optical light microscopy as well as scanning and transmission electron microscopy with their respective variations. Apart from a short overview on instrumentation, the different sample preparation techniques are explained and a selection of pharmaceutical application examples is provided to illustrate the wealth of information that can be obtained and to stimulate a more detailed exploration of the possibilities of these fascinating methods.

Keywords Optical microscopy • Polarized light microscopy • Transmission electron microscopy • Cryoelectron microscopy • Freeze-fracture • Negative staining • Scanning electron microscopy • Energy dispersive X-ray spectrometry

H. Bunjes (✉)
Institut für Pharmazeutische Technologie, Technische Universität Braunschweig, Mendelssohnstraße 1, Braunschweig 38106, Germany
e-mail: heike.bunjes@tu-braunschweig.de

J. Kuntsche
Department of Physics, Chemistry and Pharmacy, University of Southern Denmark, Campusvej 55, Odense M 5230, Denmark
e-mail: kuntsche@sdu.dk

A. Müllertz et al. (eds.), *Analytical Techniques in the Pharmaceutical Sciences*, Advances in Delivery Science and Technology, DOI 10.1007/978-1-4939-4029-5_16

1 General Remarks on Microscopy in Pharmaceutical Formulation Research

Investigation by light or electron microscopy is a very helpful tool in formulation research as it yields visual images of the objects of interest. It is particularly suitable for the investigation of samples containing particles; Scanning Electron Microscopy (SEM) is also often used to visualize the surface structure of larger objects such as tablets. The high magnification that is employed upon microscopic investigation is a great advantage but also implies that only a small portion of the sample can usually be analyzed. Thus, investigators need to be very careful in selecting their samples and areas of investigation within the microscopic specimen appropriately in order to ensure that the data they obtain is representative for the whole sample. Several specimens usually need to be prepared and different areas of a specimen to be inspected in order to achieve this goal. Moreover, (electron) microscopic methods are prone to artifacts (e.g., resulting from unfavorable specimen-beam interactions in SEM or the preparation procedures usually required for Transmission Electron Microscopy (TEM) analysis). As a further complication, many microscopic techniques lead to two-dimensional projections of three-dimensional objects which needs to be taken into consideration upon interpretation of the images. Thus, although the principle of "seeing is believing" usually acts in favor of microscopic analysis, one should not simply trust everything that appears to be revealed in a microscopic image. A sound basic knowledge about the methods including their potential pitfalls helps to employ these powerful techniques adequately and to avoid misinterpretations. This chapter can only provide a glimpse into the fascinating field of microscopic investigation and reference to specialized textbooks is recommended to those who would like to apply the methods for their research (e.g., Carlton 2011; Flegler et al. 1995; Goldstein et al. 2003; Williams and Carter 2009). As with many other techniques, microscopy often is most useful when used in combination with other methods that can provide complementary information in particular on those facts that cannot adequately be unveiled by this technique.

2 Optical Microscopy

A lot of information can be obtained about pharmaceutical samples such as powders, suspensions or emulsions by just the simplest bright-field microscope, for example about particle morphology, size and homogeneity. Despite the comparative ease of use, low demands on instrumentation and sample preparation, optical microscopy is probably one of the most underestimated analytical techniques in modern pharmaceutics.

This chapter will introduce the basic principles of optical microscopy (often also referred to as light microscopy) together with the different techniques used in

optical microscopy such as polarizing, phase contrast and differential interference contrast microscopy. Fluorescence microscopic techniques are not included as this would go beyond the scope of this chapter. Fluorescence imaging is, however, an emerging field in both biological and pharmaceutical science and the interested reader is referred to the large number of review articles focusing on fluorescence imaging (e.g., White and Errington 2005; Oheim et al. 2006; Vielreicher et al. 2013).

2.1 General Principles of Optical Microscopy

The main components of an optical microscope are the illumination source (often a halogen lamp), the condenser, the objective and the ocular (eyepiece). The general light path in an optical microscope is schematically shown in Fig. 16.1. Comprehensive information about the theory and principles of optical microscopy can be found, for example, on the websites of microscope manufacturers (e.g., www.opympusmicro.com, www.zeiss.com/microscopy).

Key parameters in microscopy are magnification and resolution. The total magnification of an optical microscope is provided by the magnification power of the objective (usually between $\times 4$ and $\times 100$) and the magnification provided by the ocular lens system (usually $\times 10$). When using an objective with a magnification power of $\times 40$ together with an ocular with $\times 10$ magnification, the total magnification will be $\times 400$. However, even the highest magnification is worthless, if the resolution is unsatisfactory. Resolution is the smallest distance between two objects where they can be clearly distinguished as two separate objects. The resolution R of the diffraction limited light microscope can be calculated by the equation introduced by Ernst Abbe (Eq. (16.1)) where R is a function of the wavelength (λ) of the light source used for sample illumination (shorter wavelengths increase the resolution), the refractive index (n) of the media between objective and sample and the half of the opening angle of the objective (Θ):

$$R = \lambda / 2\mathrm{n} \cdot \sin\theta = \lambda / 2 \cdot \mathrm{NA} \tag{16.1}$$

The product $(\mathrm{n} \cdot \sin\theta)$ is known as the numerical aperture NA of an objective and provides convenient information about resolution of a given objective. The larger the opening angle of an objective (and thus the larger its aperture), the more of the diffracted light from the sample can be gathered and the higher the resolution of the sample image. Numerical apertures of objectives for optical microscopy range from 0.1 for very low magnification objectives (e.g., $\times 4$) up to about 0.9 for high magnification objectives (e.g., $\times 100$). By replacing air by a medium with higher refractive index (e.g., water or oil, Table 16.1) between the sample and the objective, higher numerical apertures can be achieved, e.g., up to 1.6 when using an immersion oil. The oil immersion technique requires specially designed

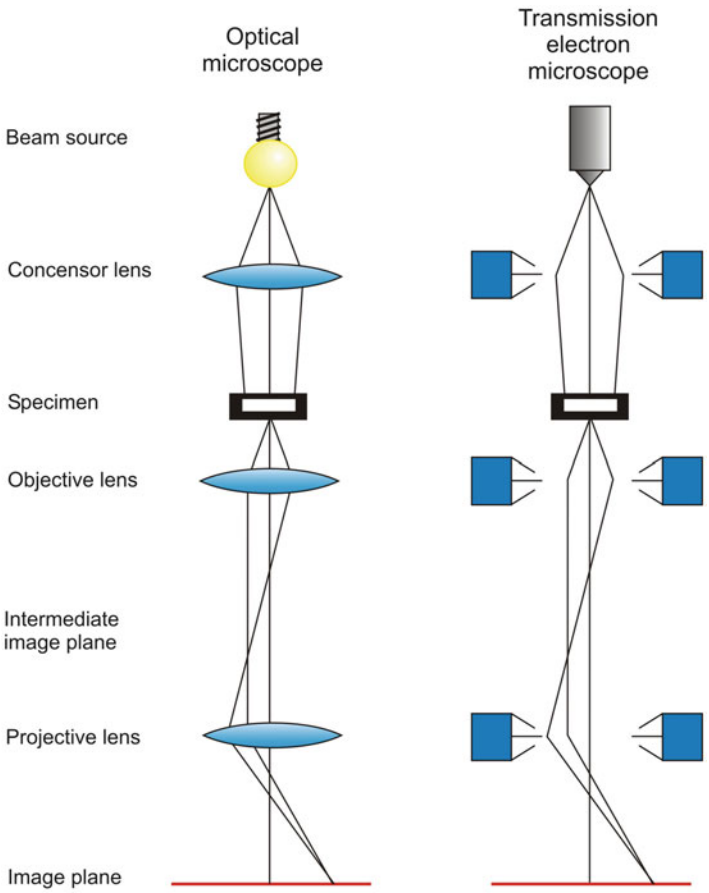

Fig. 16.1 Comparison of the setup of an (inverted) optical microscope with that of a transmission electron microscope

objectives (oil immersion objectives) and is generally used at high magnification (where a high resolution is required).

Another important characteristic of microscopic objectives is the correction for imaging errors (aberrations): Spherical aberrations (also known as aperture errors), chromatic aberrations (caused by dispersion effects) and aberrations caused by the field curvature (when using lenses with curved surface producing a curved image plane). Objectives with different degree of correction of aberrations (and consequently costs) are available (Abramowitz et al. 2002; Drent 2005; Piston 1998). Plane objectives generally provide correction for field curvature. Common types of objectives together with their degree of correction for optical aberrations, numerical aperture and magnification are summarized in Table 16.2.

Table 16.1 Common immersion media in optical microscopy (Abramowitz and Davidson 2014)

Material	Refractive index
Air	1.0003
Water	1.333
Glycerol	1.4695
Paraffin oil	1.480
Cedar wood oil	1.515
Synthetic oil	1.515

Table 16.2 Magnification, numerical aperture and working distance for common objectives (Spring et al. 2014)

Type of objective	Magnification	Numerical aperture	Working distance (mm)
Achromat correction for • SA with 1 color • CA with 2 colors	×4	0.10	30.00
	×10	0.25	6.10
	×20	0.40	2.10
	×40	0.65	0.65
	×100 (oil)	1.25	0.18
Plan achromat correction for • SA with 1 color • CA with 2 colors • FC	×4	0.10	30.00
	×10	0.25	10.50
	×20	0.40	1.30
	×40	0.65	0.57
	×100	0.90	0.26
	×100 (oil)	1.25	0.17
Plan fluorite correction for • SA with 2–4 colors • CA with 2–4 colors • FC	×4	0.13	17.10
	×10	0.30	16.00
	×20	0.50	2.10
	×40	0.75	0.72
	×100	0.90	0.30
	×100	1.30	0.20
Plan apochromat correction for • SA with 3–4 colors • CA with 4–5 colors • FC	×4	0.20	15.70
	×10	0.45	4.00
	×20	0.75	1.00
	×40	0.95	0.14
	×100 (oil)	1.40	0.13

The price of the objectives increases with increasing degree of aberration correction (SA = spherical aberration, CA = chromatic/color aberration, FC = field curvature)

The condenser is primarily an optical lens system which focuses the light from the illumination source onto the sample. It usually is composed of a diaphragm with variable aperture and one or more lenses. In the up-right transmission light microscope, the condenser is located above the light source and below the sample. For special techniques used in optical microscopy (cf. Sect. 2.2) the condenser is equipped with special optical filters. The ocular lenses (eyepiece) focus the microscopic image onto the image plane (e.g., the eye) and usually also provide an

additional magnification (often ×10). Modern microscopes are often equipped with a tri-ocular eyepiece facilitating connection to a camera. Finally, optimal illumination of the sample is a prerequisite for any convenient microscopic analysis and Köhler's illumination, introduced in 1893 by August Köhler, is still the predominant technique applied (Davidson and Fellers 2003; Goldberg 1980).

2.2 *Special Techniques in Optical Microscopy*

A limiting factor, especially with biological samples, is the poor contrast in normal bright field light microscopy. By introducing special filters in the light path, contrast of the image can be improved (phase contrast and differential interference contrast) or optical properties (birefringence) can be visualized by polarizing microscopy.

In the phase contrast technique (Elliot and Poon 2001; Pluta 1969), differences in refractive indices in sample structures are "converted" to bright-dark contrast thus providing contrast in a sample even if the differences in optical densities between the visualized structures are small. For this technique, a ring annulus is included in the condenser producing a hollow cone of light. A matching phase shift ring is located in the objective, resulting in an artificial phase difference of the light wave together with a reduction of light intensity. Due to these effects, an interference with the light that has been diffracted by the sample occurs and a phase contrast image is the result (Fig. 16.2 top). A disadvantage of the phase contrast technique is halo-formation and that it can only be used with thin samples.

A more sophisticated method to visualize samples with low contrast is the differential interference contrast setup (Elliot and Poon 2001) where differences in optical density in the sample are visualized as a difference in relief in the image (Fig. 16.2 bottom). However, the three-dimensionally appearing image is an optical effect and does not necessarily reflect the true structure of the sample. The optical setup is more complicated than that used in phase contrast microscopy and polarized light is required as light source. Special prisms (Wollaston prisms) are located in the condenser and in the objective. The prism in the condenser splits the polarized light into two beams, which have a slight difference in their traveling direction and the prism in the objective re-combines the beams. By passing the sample, both beams are affected when passing density boundaries and their optical path will be different when entering the second prism generating the differences in the relief and the three-dimensional appearance of the structure in the microscopic image.

Polarization microscopy (Oldenbourg 1996; Weaver 2003) is probably one of the most commonly used techniques of optical microscopy in the pharmaceutical field when investigating optically anisotropic (birefringent) samples such as crystalline or liquid crystalline materials. Two polarization filters are applied, one placed in the condenser (the polarizer providing polarized light for sample illumination) and another above the objective (the analyzer). The analyzer can be moved in and out of the light path and also allows adjustment of the angle respective to the

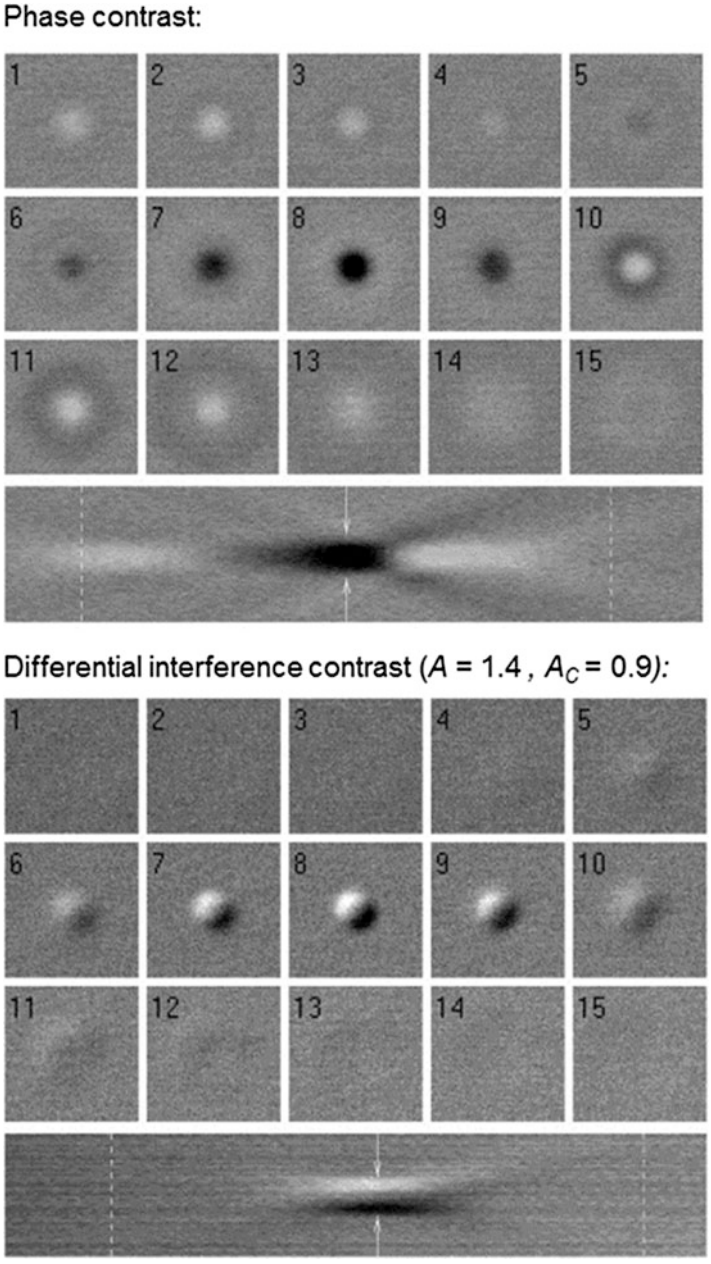

Fig. 16.2 Different contrast techniques used in light microscopy: microscopic images of a single PMMA sphere, radius $R_P = 550 \pm 7$ nm, refractive index $n_P = 1.49$, in decalin, $n_m = 1.47$. The top 15 images each (field of view 4.3 μm × 4.3 μm) form a series at varying degrees of defocus: 1.0 μm of forward axial (focusing) movement separate successive images, with no. 8 being in focus. The larger bottom images are a respective composite of 1-pixel-wide slices across the center of 165 images like the series above them, but with each separated by 0.11 μm; this gives a quasi-side-on view; image no. 8 of the upper series is at the line indicated by the arrows; the dotted lines show the positions of images 1 and 15. Reprinted from Elliot and Poon 2001, Copyright (2001), with permission from Elsevier

polarizer. If polarizer and analyzer are inserted into the optical path and the analyzer is oriented perpendicular to the analyzer (crossed polarizing filters), no light is passing when the sample is isotropic and the image appears dark. In contrast, viewing a birefringent sample, characteristic bright/dark patterns, which depend on the sample's birefringence, are observed. Often, a so-called λ-plate can be inserted in the light path just below the analyzer and the image of an isotropic sample with crossed polarizing filter will appear purple.

2.3 *Applications of Optical Microscopy in Pharmaceutical Analysis*

The pharmacopoeias, e.g., the European Pharmacopoeia (Ph.Eur.) suggest optical microscopy for the detection of sub-visible contaminations in infusions and injections (Ph.Eur. 2.9.19) and for the characterization of particles >1 μm (Ph.Eur. 2.9.37). These monographs illustrate the two major applications of optical microscopy in pharmaceutical sciences: Quality control and material science.

Simple bright-field optical microscopy can already provide important information about a pharmaceutical sample, for example to detect drug precipitation in emulsions, particulate contaminations and the presence of undesired large particles in the μm-size range in colloidal dispersions. Differential interference contrast optical microscopy has been applied for stability evaluation of w/o/w multiple emulsions where coalescence of the internal aqueous phase could clearly be detected after storage of the samples (Hoppel et al. 2014). Optical microscopy provides an important analytical tool for quality control of colloidal formulations such as nanoparticle dispersions, nanoemulsions, liposomes and so on. Colloidal drug carrier systems have been intensively studied in the last decades especially with respect to drug targeting purposes but the number of approved nanomedicines (especially based on nanoparticles as drug carriers) is still unsatisfactory. Strict control of size and size distribution combined with physical stability present a main requirement for formulations intended for intravenous injection, but adequate physicochemical characterization and the lack of generally accepted standard methods for size determination together with problems of physical stability still present a serious challenge in the development of nanomedicines (Dawidczyk et al. 2014). Although optical microscopy allows rapid detection e.g., of drug precipitation in colloidal suspensions which may not be detectable by conventional particle sizing methods based on light scattering, optical microscopy is currently only rarely described for the characterization of colloidal dispersions in the scientific literature. Driscoll and co-workers used optical microscopy in addition to light scattering methods for stability evaluation of parenteral fat emulsions (Driscoll 2006). The limitations in detecting fractions of large particles by conventional light scattering methods (e.g., laser diffraction with sub-micron instrumentation) have also clearly been seen for drug nanosuspensions (Keck and Müller 2008; Keck

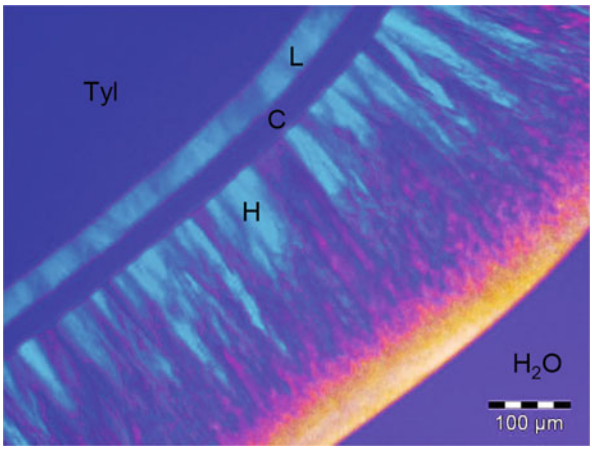

Fig. 16.3 Polarizing light micrograph of the liquid crystalline phases developing in the contact zone between the nonionic surfactant tyloxapol (Tyl) and water (H_2O): H: hexagonal; C: cubic; L: lamellar phase. Only the hexagonal and the lamellar phase exhibit birefringence

2010). These examples illustrate the usefulness of optical microscopy to get at least qualitative information about the presence of µm-particles in colloidal dispersions. For quality control and size determinations, optical microscopy should always be applied in addition to conventional light scattering methods.

The probably most frequently used application of (polarizing) optical microscopy in pharmaceutical analysis is material characterization, e.g., for the investigation of polymorphism (Bauer et al. 2001; Gilchrist et al. 2012; Nichols and Frampton 1998), crystallization behavior (Jurasin et al. 2011; Munk et al. 2012; Seefeldt et al. 2007; Tian et al. 2009; Wu et al. 2012), identification of liquid crystalline phases (Amar-Yuli and Garti 2005; Gong et al. 2011; Kuntsche et al. 2009b; Prehm et al. 2008) (Fig. 16.3) and phase behavior of mixtures (Benedini et al. 2011; Mercuri et al. 2012; Nonomura et al. 2009). In this context, microscopy is usually used in combination with other analytical techniques such as X-ray scattering/diffraction, differential scanning calorimetry and spectroscopic methods. If the microscope is equipped with a hot-stage sample holder (hot stage microscopy), phase transitions can be directly monitored and birefringence patterns observed at the different temperatures can facilitate phase identification. A comprehensive description about the use of polarizing microscopy and application of hot stage microscopy can be found in Carlton (2011).

Knowledge of solid state properties such as crystal modifications and crystal morphology are of uppermost importance as they determine, for example, solubility, dissolution rate as well as the efficiency of downstream processes such as milling (Chow et al. 2008). As an example, the influence of poly(N-isopropyl acrylamides) on the crystallization of nitrofuantoin as a model drug has recently been studied by Munk et al. (2012). Without the polymer, nitrofurantoin crystallizes from acetone-water mixtures forming needle-shaped crystals, whereas both a dendritic crystal morphology and uncontrolled crystallization of a metastable crystal modification (as identified by Raman spectroscopy) was observed in presence of the polymer (Fig. 16.4).

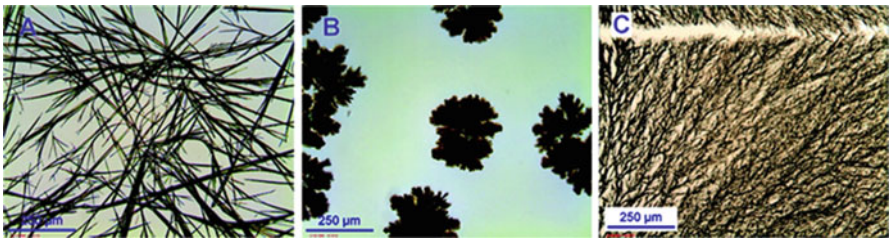

Fig. 16.4 Nitrofurantoin monohydrate (NFMH) crystallized from acetone:water mixtures in the presence of (**A**) no additive (needle growth of NFMH form II), (**B**) atactic poly(N-isopropyl acrylamide) (PNIPAM) (controlled dendritic growth of NFMH form II), (**C**) atactic PNIPAM (uncontrolled growth of NFMH form I). Reprinted with permission from Munk et al. 2012. Copyright (2012) American Chemical Society

3 Electron Microscopy

If higher resolution than achievable in light microscopy is required electron microscopic techniques can be employed to view the sample. The use of electron microscopic methods does, however, usually require more sophisticated sample preparation techniques and the sample is thus less close to its natural state upon observation. Two different types of instruments are typical for electron microscopy—transmission electron microscopes (TEMs) and scanning electron microscopes (SEMs). These two classes of instruments share some common basic features but also have fundamental differences as explained in the following.

3.1 General Setup of Electron Microscopes

Compared to a light microscope, most electron microscopes are rather large instruments. All of them consist of a microscopic column containing the electron source and the electron optical system, a sample stage or holder and detection systems that provide the data for the generation of electron microscopic images (Figs. 16.1 and 16.10). While electron beam generation and focusing are conceptually similar in TEM and SEM, the processes involved in image formation are fundamentally different. In the transmission setup, the image is detected much below the sample which is positioned in the upper part of the column. In conventional scanning electron microscopes, the sample forms essentially the lowest part of the setup and detection of the image generating data takes place in closer vicinity to and above the sample. Much shorter microscopic columns can thus be used in SEM as compared to TEM. In the following, after a short description of the common features of both types of instruments, the specificities of each technique will be outlined.

The electron beam is generated at the top of the column in an electron gun by thermionic or by field emission. For thermionic emission usually a tungsten hairpin

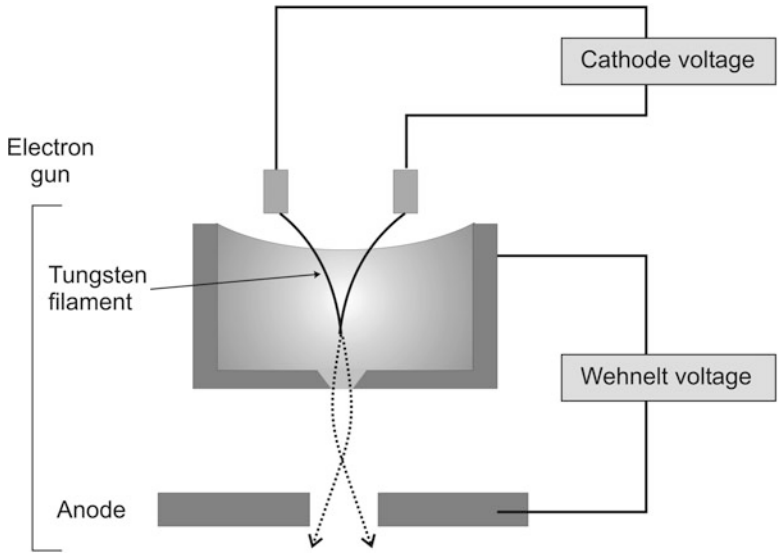

Fig. 16.5 Electron gun (filament setup) for beam generation in electron microscopes

wire (filament) or a lanthanum hexaboride (LaB_6) crystal with very fine tip is electrically heated resulting in the emission of electrons at the tip of the filament or crystal. The filament (or crystal) is operated at a very high negative potential and thus acts as a cathode (Fig. 16.5). The electrons emitted from the tip of the cathode are accelerated in an electric field towards a circle-shaped anode operated at zero potential. The electrons that pass the aperture in the center of the anode form the electron beam used for analysis. The cathode is surrounded by the Wehnelt cap set to an even higher negative potential than the cathode. Thus, the Wehnelt cap repels the electrons bringing them to a focus in front of the anode aperture. In field emission guns, electrons are "drawn" out of a very fine tungsten tip by a strong electric field applied between the emitting cathode and a first anode. The emitted electrons are accelerated toward a second anode; the potential between this anode and the cathode determines the accelerating voltage. Field emission can be accomplished in the cold or with the aid of heat to the tip (Schottky emission). Field emission guns combine high brightness of the electron beam with small beam size and narrow wavelength distribution of the emitted electrons; they are particularly useful for high resolution analysis in SEM. The costs for such instruments are, however, much higher than for those employing thermal emission.

The generated electron beam passes a set of electromagnetic lenses on its way down the column. Condenser lenses condense the beam and finally an objective lens focuses it onto the specimen. Apertures (small pieces of metal containing holes through which the beam must pass) can be used at different places of the column to e.g., shape the beam and to remove stray electrons. Usually, the whole electron microscopic setup is operated under high vacuum to avoid discharging effects due to ionization of gas molecules, scattering of the electrons as they interact with the gas molecules and, in particular, to protect the electron source from deleterious chemical reactions (e.g., oxidation) that could dramatically reduce their lifespan.

3.2 Transmission Electron Microscopy (TEM)

3.2.1 The Transmission Electron Microscope

The principal setup of a TEM (Williams and Carter 2009; Flegler et al. 1995) is similar to that of an inverted light microscope in which the sample is, however, illuminated by an electron beam focused by electromagnetic lenses (Fig. 16.1). Electrons that pass the specimen are projected onto a viewing screen or a photographic or electronic image recording device. Adequate sample preparation is a very important part of electron microscopic investigation by TEM. Since electrons cannot easily penetrate matter, only very thin samples can be studied. The contrast in TEM is obtained by the interaction of the electrons with the material (scattering). Heavy metals like lead, uranium and platinum strongly interact with the electrons and are, therefore, often used to improve the contrast (e.g., upon negative staining, see below). Since increasing acceleration voltage decreases the wavelength of the electrons the resolution of TEM becomes better at higher voltages. On the other hand, the contrast decreases with increasing acceleration voltage as the scattering of the electrons is inversely proportional to their velocity. In TEM investigations on colloidal drug carrier systems voltages between 80 and 200 kV are usually applied.

3.2.2 Sample Preparation and TEM Investigation

Negative staining is the most straightforward preparation method for the evaluation of colloidal particles by TEM (Friedrich et al. 2010; Harris 1997, 2007). A small drop of liquid sample is positioned on a TEM grid (small gold or copper grid with defined mesh size coated e.g., with a thin layer of carbon) which usually has been subjected to glow discharge in order to hydrophilize the carbon support film. During a short time of contact, particles present in the sample adsorb to the carbon support. After blotting excess sample and optional washing with water, a staining solution containing heavy metal salts which provide high contrast in the electron microscope (e.g., uranyl acetate, ammonium molybdate, or sodium phosphotungstate) is contacted with the grid. Excess solution is removed from the grid and the sample is air dried at room temperature. Dry samples can either be stored or directly be investigated in the electron microscope. Upon TEM observation, the colloidal particles appear bright against the darker background of the stain which interacts more strongly with the beam electrons than the usually organic matrix of the particles under investigation. Although the dried film of stain provides some sort of support for the colloidal particles, both staining and drying may result in structural alterations of the colloids which always need to be taken into consideration when interpreting negative staining TEM images. In particular “soft” particles like liposomes or emulsion droplets tend to collaps during sample preparation (Friedrich et al. 2010; Klang et al. 2013).

A closer approach to the native state of the particles is obtained when using freeze-fracturing (Severs 2007). This technique relies on the vitrification (i.e., transformation into the glassy state) of the liquid components of the sample (e.g., the aqueous dispersion medium) by extremely rapid cooling. The liquid sample is sandwiched between two copper or gold holders and subjected to freezing e.g., in liquid propane or melting nitrogen. This can be done manually or by using specialized equipment like a cryojet device. Under constant cooling in liquid nitrogen, the frozen sample is transferred to a freeze-fracturing unit where it is fractured under continued cooling and in high vacuum. The fracture planes develop predominantly along areas of the sample with weak molecular interactions (e.g., within lipid bilayers) (Meyer and Richter 2001). In order to obtain an observation plane with higher structuring the fractured sample can optionally be etched by water sublimation in vacuum leaving behind the non-volatile components of the sample. Afterwards, the sample surface is shadowed with a thin platinum/carbon layer (about 2 nm) usually at an angle of 45° with respect to the fracture surface. Subsequently, a thicker carbon layer (about 20–30 nm) is deposited onto the sample at an angle of 90° to improve stability of the film deposited on the sample surface. The sample is removed from the freeze-fracture device and the original sample cleaned away by rinsing with solvents to remove all organic residues. Thus, a "negative" replica of the fractured (and etched) sample plane is obtained that is placed on an electron microscopic grid to be viewed in the electron microscope. Due to the shadowing the images may adopt a somewhat "three-dimensional" appearance. The platinum/carbon replicas are stable over time and upon TEM observation; thus, they can be stored for later re-investigation. When obtained under optimal sample preparation conditions, freeze-fractured replicas reflect the original, native state of the sample and can provide valuable insights also into the interior of particles. Artifacts may, however, easily occur, e.g., due to an insufficient freezing rate that may induce crystallization or as a result of re-deposition of solvent molecules onto the sample plane after fracturing. Moreover, due to the many steps involved, sample preparation by freeze-fracturing is an intricate and rather time-consuming technique. With the more widespread availability of cryo-TEM instruments it has been replaced by this technique to some extent, although it remains an important source of ultrastructural information.

Investigation by cryo-TEM after plunge-freezing is the closest approach to the native state of the samples. After vitrification, colloids can directly be studied in their frozen-hydrated state. This way, information about the size, shape and internal structure of the particles may be obtained (Klang et al. 2012, 2013; Kuntsche et al. 2011). In contrast to the above mentioned techniques, which essentially rely on the preparation of suitable specimens, sample investigation by cryo-TEM additionally requires specialized electron microscopic equipment (see below). Detailed information on this technique can be taken from a large pool of dedicated literature (Friedrich et al. 2010; Grassucci et al. 2007, 2008; Harris 1997).

In most cases, specialized carbon-coated holey grids are used in cryo-TEM studies. Such grids consist of a squared copper mesh covered with a carbon-coated foil which is perforated by holes that can have different shapes. After fixation of the

TEM grid (previously submitted to glow discharge to hydrophilize the carbon) in the preparation chamber, a small droplet of sample is applied. Upon removal of excess sample by blotting with a filter paper a thin film of the sample forms in the holes of the grid (the sample must not be too viscous for this procedure). The sample is then immediately plunge-frozen, commonly in liquefied ethane cooled to liquid nitrogen temperature. As in freeze-fracturing, a very high cooling rate is required to vitrify the sample thereby avoiding the formation of crystalline ice. Automated vitrification systems with controlled humidity and/or temperature are available that help to ensure a reproducible sample preparation procedure (Egelhaaf et al. 2000). Under constant cooling, the grid with the vitrified sample is removed from the liquid ethane, excess ethane is blotted off and the sample is transferred into the cooled sample holder which is then quickly inserted into the electron microscope. Sample preparation for cryo-TEM thus requires strict control of sample environment over the whole process of preparation, transfer and electron microscopic investigation. Contact with atmospheric moisture needs to be avoided as it may lead to a contamination with ice on the vitrified specimen and/or on cooled parts of the equipment.

Apart from a specialized cryo-holder that ensures continuous cooling of the sample to about liquid nitrogen temperature upon microscopic observation the cryo-TEM should be equipped with a liquid nitrogen-cooled decontaminator close to the sample holder that collects water molecules being introduced into the vacuum system with the cooled holder or evaporating from the sample during observation. Often, cryo-holders allow tilting of the sample during observation thus providing access to information about the three-dimensional structure of the particles of interest which can be investigated from different angles (Barauskas et al. 2005; Kuntsche et al. 2010b). Sophisticated data evaluation even allows the reconstruction of the three-dimensional particle structure (Koning and Koster 2009). The colloidal structures embedded in the thin vitrified film are viewed under low dose conditions to avoid electron beam damage. In spite of this, the time period for viewing of the sample in cryo-TEM is often rather limited as most samples are sensitive to radiation.

Also in cryo-TEM artifacts may occur (Friedrich et al. 2010; Kuntsche et al. 2011; Burrows and Penn 2013). For example, cryogen residues can remain from the plunge-freezing process or there may be ice contamination due to a too high content of evaporated water in the microscopic column. Since the sample film usually becomes thinner in the middle of a hole of the grid, smaller particles are usually found in the middle part of the film. Very large particles may already be removed upon blotting when preparing the thin film to be vitrified.

3.2.3 Application of TEM in Pharmaceutical Formulation Research

TEM is particularly useful for the study of colloidal and nanostructured drug delivery systems. Often, the different preparation techniques are used in combination to obtain complementary information (Figs. 16.6 and 16.7). A lot of application

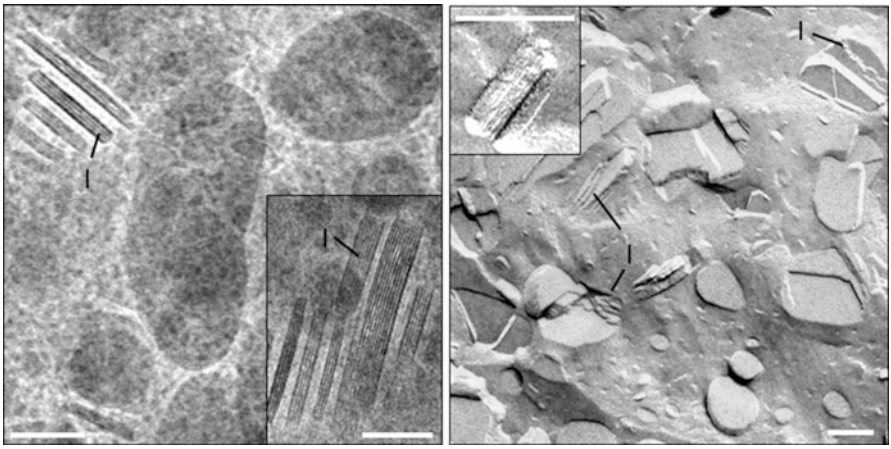

Fig. 16.6 Cryo (left) and freeze-fracture (right) transmission electron micrographs (bars represent 100 nm) of tristearin nanoparticles in the β-modification. The particles, which have a platelet-like shape, appear as elongated ellipsoidal structures in top-view and long rectangles in side-view. They display a layered internal structure (l) and tend to pack in stacks at this concentration (10 % triglyceride). Reprinted with permission from Bunjes et al. 2007. Copyright (2007) American Chemical Society

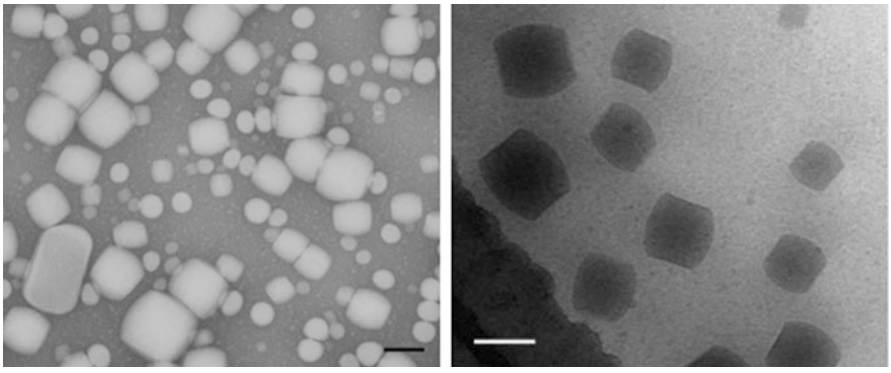

Fig. 16.7 TEM micrographs of supercooled cholesteryl myristate nanoparticles stabilized with polysorbate. The particles have a cylindrical shape that appears spherical in top-view and rectangular in side-view. Left: negative staining, scale bar: 140 nm; right: cryo-TEM, scale bar: 100 nm. Data from Kuntsche et al. 2010b

examples on pharmaceutically relevant systems can be found in extensive reviews on the use of transmission electron microscopy in pharmaceutical research (Klang et al. 2012, 2013; Kuntsche et al. 2011) and only a selection is presented in the following.

As a prominent example, the size, shape and lamellarity of liposomes have intensively been studied with TEM techniques (Almgren et al. 2000; Bibi et al. 2011; Hope et al. 1989). Structural alterations due to differences in bilayer

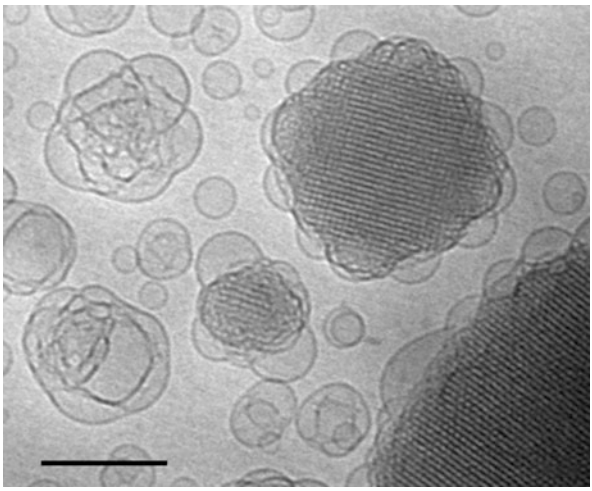

Fig. 16.8 Cryo-TEM micrograph showing the different colloidal structures in an aqueous dispersion of glycerol monooleate/poloxamer 407 after high pressure homogenization: Vesicles, cubic phase nanoparticles and particles of intermediate structure. Scale bar: 200 nm. Data from Kuntsche et al. 2008

composition and physical state can easily be visualized this way as can drug precipitation within liposomes as a result of gradient loading (Kuntsche et al. 2010a; Lauf et al. 2004; Li et al. 1998). Apart from liposomes, which originate from the liquid crystalline lamellar phase, nanoparticles based on other types of lyotropic mesophases, in particular the cubic and hexagonal phase, are being increasingly investigated in the field of drug delivery. Cryo-TEM is an invaluable characterization method for the corresponding dispersions, as it allows detailed visualization of the shape and the internal structure of the nanoparticles (Barauskas et al. 2005) (Fig. 16.8). This technique is even more important for characterizing internally structured nanoparticles without a periodic internal pattern ("sponge" nanoparticles), where the structure cannot be elucidated in detail by other methods (Barauskas et al. 2006). The cage-like ultrastucture of immunostimulating complexes (Iscoms) and related colloidal structures, that have an interesting potential as vaccine adjuvants, have intensively studied with TEM, in particular after negative staining (Demana et al. 2004; Madsen et al. 2010; Muhsin et al. 1989). The structure of complexes resulting from interaction of nucleic acids with cationic lipids, surfactants or polymers is well accessible to studies with cryo- and freeze-fracture TEM (Ainalem et al. 2009; Alfredsson 2005; Sternberg et al. 1994). Cryo-TEM in particular has also been employed to identify the various colloidal structures that may be formed by amphiphilic block copolymers (spherical and worm-like micelles, vesicles) being under investigation as alternative drug carrier systems (Rank et al. 2009; Velluto et al. 2008).

The different colloidal structures (e.g., emulsion droplets, vesicles formed by excess phospholipid) occurring in colloidal fat emulsions for parenteral nutrition or as drug carriers have also been studied by TEM techniques (Klang et al. 2012; Kuntsche et al. 2009a; Westesen and Wehler 1992). Moreover, TEM has led to valuable insights into the structure and morphology of solid lipid nanoparticles. Anisometric, platelet-shaped particles usually form upon crystallization of

spherical triglyceride nanodroplets after processing by melt-homogenization but other particle shapes (ranging from spherical over block-like to the often occurring platelets) may be observed in dependence on the composition and preparation process (Bunjes et al. 2007; Finke et al. 2013; Rosenblatt and Bunjes 2009). At higher concentration, platelet-like particles tend to self-organize in stacks (Bunjes et al. 2007; Unruh et al. 2002) (Fig. 16.6). Under favorable circumstances, even the lamellar organization of the triglyceride molecules within single crystalline particles can be observed (Bunjes et al. 2007; Rosenblatt and Bunjes 2009) (Fig. 16.6) Upon incorporation of liquid oils or drugs, liquid compartments sticking to the surface of the solid, platelet-like matrix of the nanoparticles may be formed as revealed by TEM images (Bunjes et al. 2001; Jores et al. 2004). Also the association of inorganic sunscreen pigments with solid lipid nanoparticles could be visualized (Villalobos-Hernández and Müller-Goymann 2005).

As a kind of intermediate between liquid emulsion droplets and solid lipid nanoparticles lipid nanoparticles in the supercooled smectic state have been prepared from cholesterol esters as drug delivery system for poorly water-soluble drugs. TEM studies revealed that—depending on the nature of the emulsifier used—these particles are of more or less clear cylindrical shape (Kuntsche et al. 2004, 2005, 2010b) (Fig. 16.7). Also for these dispersions, the presence of other colloids formed by the excess of emulsifier(s) could be observed in co-existence with the smectic lipid nanoparticles.

Examples for the use of TEM also include studies on nanoparticulate dispersions of pure drugs or drug conjugates. Examples are the visualization of the shape of amorphous and crystalline felodipine nanoparticles by cryo-TEM, cryo- and freeze-fracture TEM studies on supercooled ubidecarenone nanoparticles or the detection of shell-enclosed hexagonally structured nanoassemblies in aqueous dispersions of a gemcitabine squalene conjugate by cryo-TEM (Couvreur et al. 2008; Lindfors et al. 2007; Siekmann and Westesen 1995). Crystalline drug nanoparticles can be visualized in a rather straightforward manner by investigation of negatively stained specimens (Bitterlich et al. 2014) (Fig. 16.9).

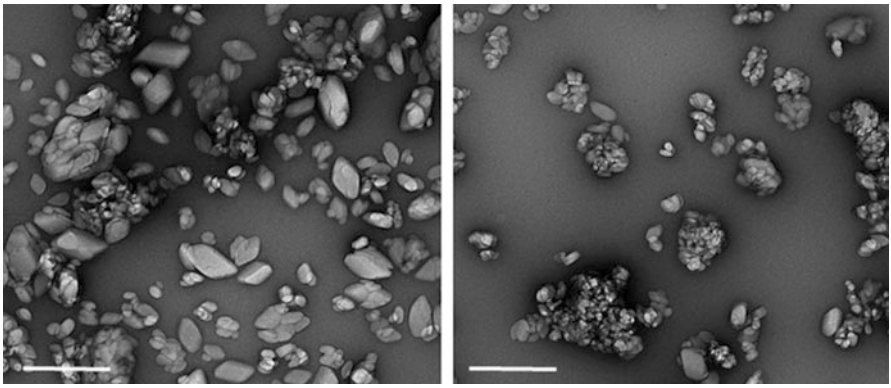

Fig. 16.9 TEM micrographs (negative staining) of a fenofibrate nanosuspension after 8 h (left) and 24 h (right) of grinding in a stirred media mill. Scale bars: 500 nm. Data from Bitterlich et al. 2014

In contrast to negative staining and cryo-TEM, TEM after freeze-fracturing can also be employed on semisolid and even solid systems. Thus, it has been used for the investigation of different kinds of liquid crystalline structures, vesicular phospholipid gels or semisolid emulsion systems as well as for solid lipid matrices (Attama et al. 2006; Brandl et al. 1997; Gašperlin et al. 1994; Müller-Goymann 1984; Paspaleeva-Kühn and Nürnberg 1992; Rades and Müller-Goymann 1997; Savic et al. 2005; Schütze and Müller-Goymann 1992).

3.3 Scanning Electron Microscopy (SEM)

Scanning electron microscopy (SEM) is a well established tool to investigate the morphology of particles and the topology of pharmaceutically relevant surfaces at high resolution. Although it may sometimes be operated at magnifications not much higher than those used in light microscopy the considerably higher depth of field provided by SEM allows unique insight into topological features of a sample. The SEM technique relies on the generation of a very fine electron beam that scans the sample surface in a point-wise, regular manner. The beam electrons penetrate the surface of the specimen and lead to a multitude of interactions with the sample atoms. These interactions give rise to the generation of different kinds of radiation (in particular electrons and X-rays) from the specimen surface that can be monitored by specialized detectors and used for imaging and element analysis. The most important SEM technique for pharmaceutical applications is surface imaging based on the detection of secondary electrons. This technique leads to the well-known "three-dimensional" grayscale images often included in monographs on pharmaceutical excipients (e.g., Rowe et al. 2009) and scientific publications on particulate pharmaceutical formulations. This section of the chapter will introduce the basics of the method and its applications with a particular focus on imaging by secondary electron detection. For more detailed insights, a lot of specialized literature is available, in particular with reference to biological and materials science but also with regard to pharmaceutical applications (e.g., Carlton 2011; Flegler et al. 1995; Goldstein et al. 2003; Klang et al. 2013).

3.3.1 The Scanning Electron Microscope

A sketch of a typical SEM-setup is provided in Fig. 16.10. SEMs are operated at lower accelerating voltages than TEMs. The accelerating voltage may be as high as 30 kV but SEMs that can operate at voltages below 1 kV are increasingly being used. Upon passage through the microscopic column the electron beam is condensed, and finally an objective lens focuses it as a small spot onto the specimen. Scan coils, which are usually situated within the objective lens, can deflect the beam and are used to move the beam spot in a raster pattern over the surface of the specimen. Magnification depends on the dimensions of the area scanned during

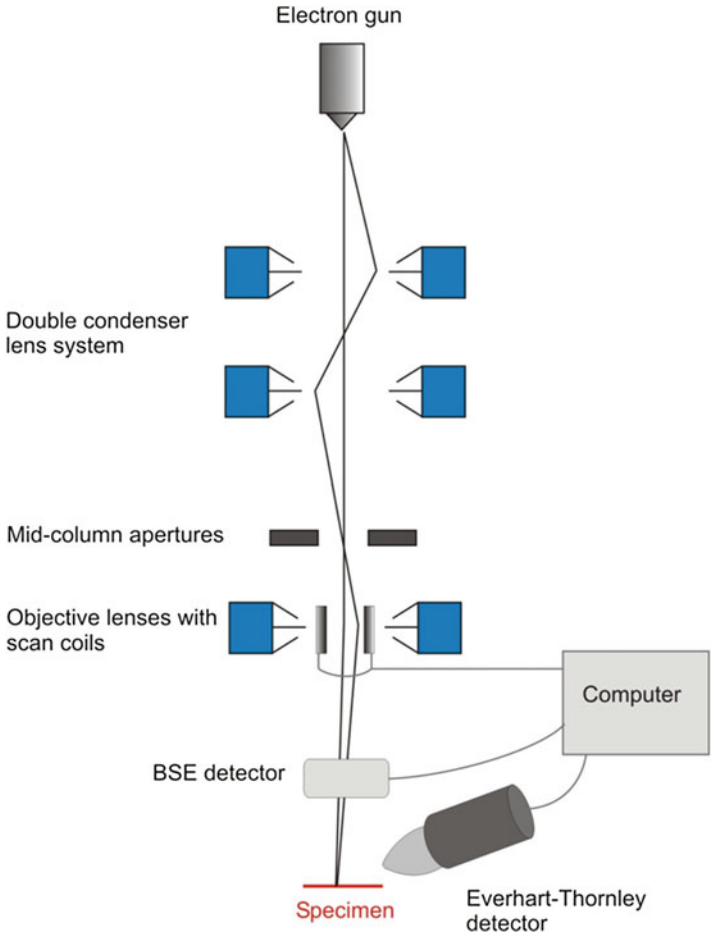

Fig. 16.10 Schematic illustration of the setup of a Scanning Electron Microscope

sample analysis (for higher magnification, the area is reduced). In order to achieve a high resolution, the spot size of the beam should be small (although spot size is not the only parameter determining resolution of a SEM). Interaction of the electron beam with the atoms of the specimen induces a multitude of effects (see Sect. 3.3.2). The resulting signals arising from the specimen's surface are recorded by corresponding detectors which are synchronized with the movement of the beam spot. Thus, the type or strength of a detector signal can be allocated to the corresponding position of the specimen's surface where the effect was produced. The release of so-called secondary electrons (SE) from the specimen is used for surface imaging. SE have a rather low energy and are monitored by a detector positioned at the side of the sample chamber. Usually, an Everhart-Thornley detector is used for this purpose (Fig. 16.11). The front structure (Faraday cage or collector screen) of this detector is positively charged (~300 V) and can thus collect

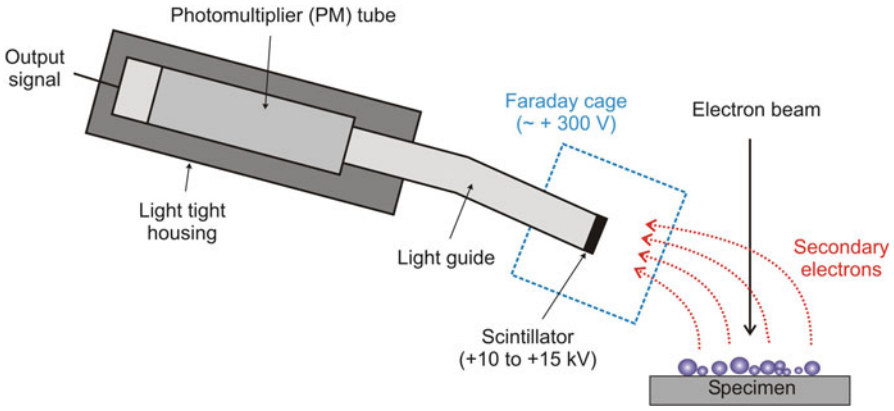

Fig. 16.11 Operating principle of an Everhart-Thornley detector

the low-energy SE emerging from anywhere on the specimen surface by electrostatic attraction. High energy electrons are not deflected by the relatively low potential of the Faraday cage and will only be detected if their path sends them directly into the opening of the detector. Electrons inside the Faraday cage are accelerated by a very high positive potential onto a small scintillator disc where they induce photon formation. By a light pipe, the photons are directed to a photomultiplier localized outside of the specimen chamber. Here, they cause the formation of an electron cascade thus amplifying the signal which is finally recorded and assigned to the respective spot on the specimen surface.

3.3.2 Electron Beam-Specimen Interactions

After entrance into the sample, the beam electrons undergo a multitude of interactions upon collision with the atoms of the sample. Thus, they get scattered, change direction and lose energy on their way. The interactions occur in a so-called interaction volume which has a pear- or droplet-like shape (Fig. 16.12). The size of the interaction volume increases with accelerating voltage and decreases with increasing atomic number. Within the interaction volume, the electrons undergo elastic or inelastic interactions with the sample atoms. Elastic interactions occur due to interaction with the nucleus of the specimen atoms. They do not cause much change in the energy of the electrons but lead to a deflection effect at a large angle. Elastic interaction may cause the electrons to be scattered back towards the direction of the primary beam (backscattered electrons, BSE). Due to their high energy, BSE can leave the specimen from a comparatively large depth of the interaction volume.

Inelastic interactions are due to interactions with the electron shell of the specimen atoms. They cause a large energy loss of the incident electron and its deflection at low angles. Inelastic interaction may lead to the release of weakly

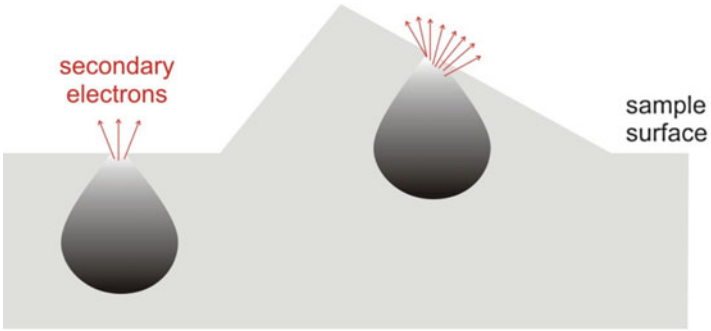

Fig. 16.12 Illustration of the pear-shaped interaction volume in which the different types of radiation that lead to image formation in SEM are created. Secondary electrons (SE) can leave the specimen only from areas close to the surface; thus, protruding parts of the specimen lead to a higher intensity in SE imaging

bound electrons from the orbital shell of the specimen atoms (secondary electrons, SE). Although SE may be generated throughout the interaction volume, only those in close vicinity (in the order of several nm) to the specimen surface can leave the specimen because of their low energy. In areas protruding from the sample surface, the fraction of SE that can leave the surface of the specimen is higher than in flat areas because more SE are generated at a distance close to the surface (Fig. 16.12). Therefore, the protruding areas appear brighter in the projection and an image of three-dimensional appearance is created. The topography of the sample is thus very well reflected in SE micrographs. The confinement of the origin of the SE created at the beam spot to a very narrow space leads to a high resolution of SE micrographs. The yield of SE increases with decreasing energy of the beam since the probability of interactions of the beam electrons with electrons from the outer shell of the specimen atoms increases when the beam electrons become slower. Thus, the resolution of surface images becomes better when the acceleration voltage is decreased. SE can also be generated by processes other than those outlined above. For example, BSE may liberate SE from other places in the specimen or even from components of the specimen chamber. Such effects decrease resolution but cannot be completely avoided.

BSE are not just a source of noise in SE micrographs but they can themselves be used for imaging. Images created from BSE detection do not reflect the surface topography in detail but can be used to analyze the composition of the sample surface. The yield of BSE generally increases with atomic number of the sample atoms albeit not in a linear manner. The intensity of electron backscattering thus reflects the sample composition. Organic materials composed solely of light atoms such as C, H, O, and N do not give rise to much backscattering. However, if components of higher atomic number are contained in the sample (for example, calcium phosphate as filling agent or API salts with inorganic counterions) contrast between areas of different composition, e.g., on a tablet surface, may be achieved

(Carlton 2011). BSE are detected close to the point where the electron beam enters the specimen chamber. As they can leave the specimen from a rather large part of the interaction volume and thus further away from the beam spot, the resolution of the corresponding images is lower than with SE detection.

3.3.3 Sample Preparation for SEM

The size of samples used for SEM is mainly limited by the size of the sample chamber; thus, samples can be rather large. In conventional SEM, sample thickness is not a problematic issue as only the sample surface is investigated. Sample preparation is often more straightforward in SEM compared with TEM. Dry powder or granule samples are usually mounted onto the sample holder of the SEM by using double-sided carbon adhesive tape (conductive). Powders can be sprinkled onto the tape or blown to it with the aid of an airstream. Also larger objects like tablets can be fixed by tape or they can be glued to the holder. To investigate the interior of tablets or larger particles, these objects may be broken or cut (preferably with a microtome). If particles agglomerate too strongly, they can be dispersed in a suitable volatile non-solvent and sprayed onto the holder or be deposited by filtration (e.g., using a Nuclepore filter). Filtration followed by drying is also well suitable for the preparation of particles from suspensions.

If the sample is non-conducting (as are most samples of pharmaceutical interest) it needs to be coated with a thin conductive layer unless investigated at very low accelerating voltage or in a low vacuum instrument. In most cases, sputter coating is used for that purpose. A sputter coating device (Fig. 16.13) consists of a vacuum-tight chamber containing an anode that holds the specimen to be coated and a cathode with the coating material (e.g., gold, palladium, carbon). After evacuation, the chamber is filled with argon gas and an electric field is generated between anode and cathode. At sufficiently high voltage an argon plasma is formed in which the argon atoms are ionized and accelerated towards the cathode. There, they liberate atoms from the coating material which distribute in the chamber and are deposited on the specimen. The process has to be controlled such that a thin (up to a few nm), continuous film is formed on the specimen; the film must not get too thick as it otherwise might cover details of the specimen's surface.

3.3.4 Environmental Scanning Electron Microscopy

Traditionally, the whole system of the SEM enclosing the electron beam (electron gun, column and sample chamber) operates under high vacuum. During the last decades, instruments that work with low vacuum in the sample chamber have become available. As these may help to overcome problems with charging of non-conducting samples and with vacuum sensitive samples they are used in some pharmaceutical applications. For example, so-called Environmental Scanning Electron Microscopes (ESEM) can operate under relatively high water vapor

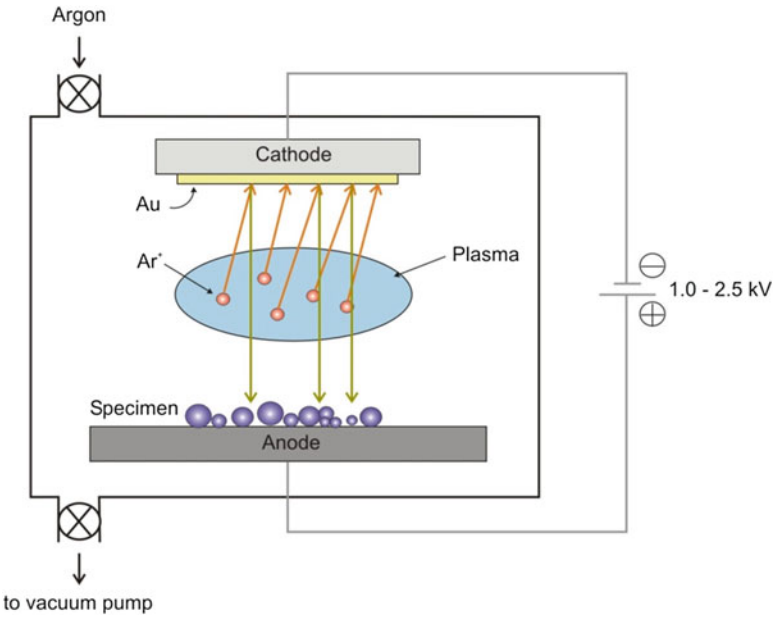

Fig. 16.13 Layout of a sputter coating device

pressures in the sample chamber but other low-vacuum devices have also been developed. Operation under low vacuum does not only allow investigating samples in a hydrated state close to ambient conditions but can also eliminate the need to coat samples with a conductive layer.

3.3.5 Energy Dispersive X-ray Spectrometry

Investigation of a sample by SEM cannot only lead to images but also to specific information on the chemical composition of the sample at specific sites. This type of investigation—energy dispersive X-ray spectrometry (EDX, often also referred to as EDS)—is based on the generation of X-rays upon interaction of the electron beam with the sample atoms. Apart from a continuous spectrum of X-rays ("Bremsstrahlung") generated by the deceleration of the beam electrons due to interaction with the specimen atoms sharp X-ray signals are produced at wavelength positions that are specific for a given element. These signals are the basis for elemental mapping by EDX. They are generated when an inner shell electron of the specimen atom is hit by the electron beam and knocked out of its position. Its space is filled with an electron from a higher energy level electron shell and the energy difference is emitted as an X-ray photon with the corresponding energy. Replacement of the electron in the innermost shell (the K shell) can occur from the next higher level shell (the L shell) leading to K_α radiation or—less probably—from the even higher M shell yielding a smaller peak of the K_β radiation. There are also electron

transitions between the higher level shells (if present) altogether leading to a more or less complex spectrum of element-characteristic, sharp signals arising on top of the continuous spectrum. The X-ray detector records the X-ray spectra arising from the areas of interest in the specimen and the characteristic signals can be assigned to the corresponding elements.

3.3.6 Pharmaceutical Application of SEM and SEM/EDX

SEM imaging is extremely helpful to examine the size, shape and detailed morphology of particles and to understand morphology-related properties of substances, formulations or dosage forms (e.g., reviewed by Schmidt (2002)). The technique is thus abundantly used in the context of research and development especially on solid dosage forms and only a very limited number of examples can be referred to here. In the evaluation of pharmaceutical raw materials (drug substances and excipients) SEM images revealing the size, shape and morphology of the particles help to understand the processing properties and pharmaceutical performance of these materials (Kleinebudde 1997; Pitchayajittipong et al. 2010). The impact of different preparation procedures like precipitation or milling on important properties of the resulting drug or excipient particles can be investigated by SEM (Crisp et al. 2011; Ho et al. 2012; Kubavat et al. 2012; Otte and Carvajal 2011; Rasenack and Müller 2002). The structure of spray and freeze dried formulations is often examined with this method (Corveleyn and Remon 1997; Devi and Williams 2013; Littringer et al. 2013; Vehring 2008) (Fig. 16.14). The formation of interactive powder mixtures, where smaller particles (usually those of the active

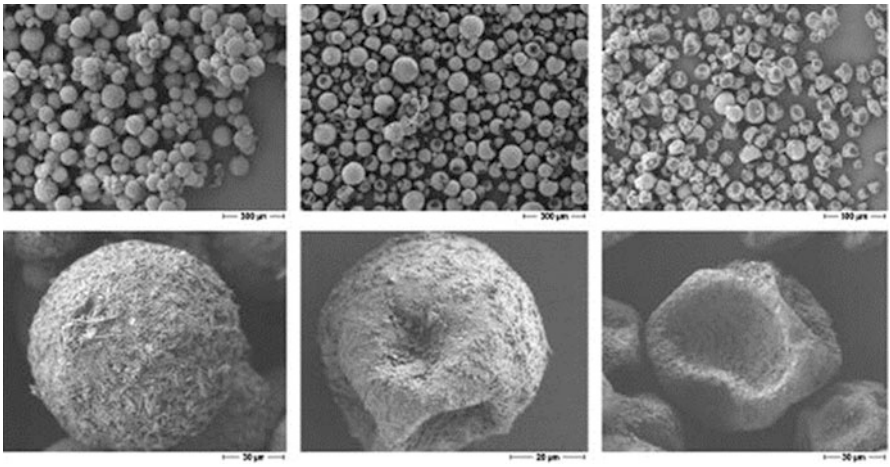

Fig. 16.14 SEM micrographs of mannitol samples spray dried at different outlet temperatures (left: 67 °C; middle: 84 °C; right: 102 °C. Scale bar 300 µm (top line), 30 µm (bottom left and right) 20 µm (bottom middle)). Reprinted from Littringer et al. 2013, Copyright (2013), with permission from Elsevier

substance) adhere to larger ones can easily be shown by SEM (Adi et al. 2007; Grasmeijer et al. 2013). Such interactive mixtures are highly relevant in formulations used in dry powder inhalers for which also other types of formulations are developed with the aid of SEM investigations (Healy et al. 2014; Hoppentocht et al. 2014). Images of tablet surfaces or cross-sections are very illustrative for the interpretation of deformation processes during tableting (Ghanam et al. 2010; Narayan and Hancock 2003) (Fig. 16.15). Similar images help to understand the

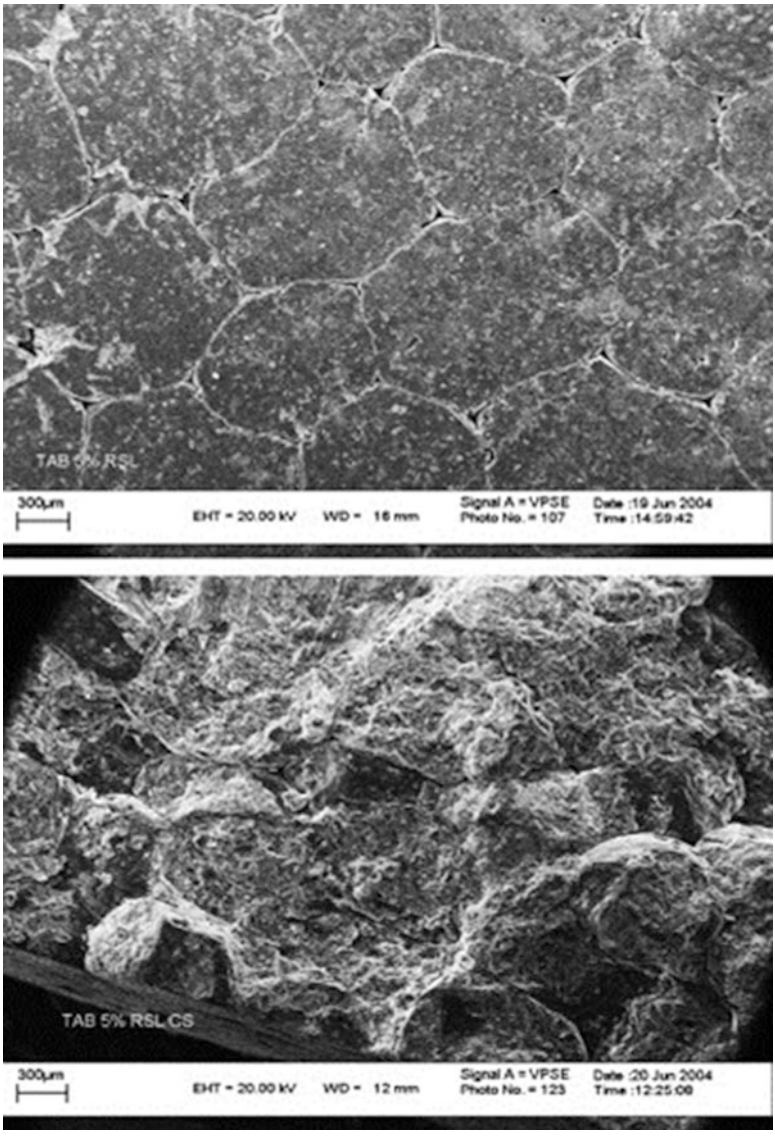

Fig. 16.15 SEM micrographs of a tablet prepared from ibuprofen-containing pellets coated with Eudragit; top: tablet surface, bottom: cross-section. Reprinted from Abbaspour et al. 2008, Copyright (2007), with permission from Elsevier

structure and formation of polymer layers upon coating of tablets, granules or other particles and their behavior upon processing (Abbaspour et al. 2008; Haaser et al. 2013; Jeong and Park 2008). In the field of parenteral dosage forms, the influence of production parameters on the morphology of polymer microparticles can be investigated and the structure and degradation of implants be analyzed (Cheng et al. 2009; Jeyanthi et al. 1996; Lee et al. 2012; Witt and Kissel 2001). SEM has also been applied to investigate particulate objects with sizes in the nanometer range, for example, to reveal the size and shape of the particles in drug nanosuspensions or of drug carrier nanoparticles (Bhakay et al. 2011; Finke et al. 2013; Gaumet et al. 2007; George and Ghosh 2013). In order to study "soft" structures in a close to their native situation a freeze-fracture technique (partly performed within the SEM instrument) is available and has been applied to lyotropic liquid crystalline cubic structures as well as other types of aqueous colloidal systems (Krauel et al. 2007; Rizwan et al. 2007).

For specific questions, the use of SEM in combination with energy dispersive X-ray spectrometry (SEM/EDX) can be a very interesting option. The possibility to identify particles or zones according to their elemental composition has, for example, been used to investigate the distribution of active ingredients or excipients in different kinds of solid dosage forms (Ghalanbor et al. 2010; Nagy et al. 2012; Pingali and Mendez 2014; Raijada et al. 2013; van Eerdenbrugh et al. 2008). In these studies, the components of interest are identified by mapping the occurrence of a substance-specific element as indicator (e.g., sulfur for spironolactone, piroxicam or proteins, or Mg for magnesium stearate). There are also approaches to map a larger number of components, e.g., present at a tablet surface, by indentifying phases of different composition using complex evaluation procedures (Scoutaris et al. 2014). Moreover, SEM/EDX analysis has proven to be an effective tool for the identification of foreign matter particles in tablets or drug nanosuspensions (Juhnke et al. 2012; Pajander et al. 2013).

4 Conclusion

Various microscopic techniques are available for the research on pharmaceutical formulations. They range from rather simple light microscopy to very advanced (and expensive) electron microscopic methods. Depending on the type of sample and question to be solved the right technique has to be chosen; however, different microscopic methods can often provide valuable complementary information. In particular for the more advanced techniques a certain degree of expertise is required in order to select the right preparation and measurement conditions for a given sample and to avoid misinterpretation of results. When used appropriately, microscopy can be extremely helpful to elucidate pharmaceutically relevant features of a sample as illustrated by numerous examples from the literature.

References

Abbaspour M, Sadeghi F, Afrasiabi Garekani H (2008) Design and study of ibuprofen disintegrating sustained-release tablets comprising coated pellets. Eur J Pharm Biopharm 68:747–759

Abramowitz M, Davidson MW (2014) Immersion media. http://www.olympusmicro.com/primer/anatomy/immersion.html. Accessed 30 Nov 2014

Abramowitz M, Spring KR, Keller HE, Davidson MW (2002) Basic principles of microscope objectives. BioTechniques 33:772–781

Adi H, Larson I, Stewart PJ (2007) Adhesion and redistribution of salmeterol xinafoate particles in sugar-based mixtures for inhalation. Int J Pharm 337:229–238

Ainalem M, Carnerup AM, Janiak J, Alfredsson V, Nylander T, Schillén K (2009) Condensing DNA with poly(amido amine) dendrimers of different generations: means of controlling aggregate morphology. Soft Matter 5:2310–2320

Alfredsson V (2005) Cryo-TEM studies of DNA and DNA–lipid structures. Curr Opin Colloid Interf Sci 10:269–273

Almgren M, Edwards K, Karlsson G (2000) Cryo transmission electron microscopy of liposomes and related structures. Coll Surf A 174:3–21

Amar-Yuli I, Garti N (2005) Transitions induced by solubilized fat into reverse hexagonal mesophases. Colloids Surf B 43:72–82

Attama A, Schicke B, Müller-Goymann CC (2006) Further characterization of theobromae oil–beeswax admixtures as lipid matrices for improved drug delivery systems. Eur J Pharm Biopharm 64:294–306

Barauskas J, Johnsson M, Tiberg F (2005) Self-assembled lipid superstructures: beyond vesicles and liposomes. Nano Lett 5:1615–1619

Barauskas J, Misiunas A, Gunnarsson T, Tiberg F, Johnsson M (2006) "Sponge" nanoparticle dispersions in aqueous mixtures of diglycerol monooleate, glycerol dioleate, and polysorbate 80. Langmuir 22:6328–6334

Bauer J, Spanton S, Henry R, Quick J, Dziki W, Porter W, Morris J (2001) Ritonavir: an extraordinary example of conformational polymorphism. Pharm Res 18:859–866

Benedini L, Schulz EP, Messina PV, Palma SD, Allemandi DA, Schulz PC (2011) The ascorbyl palmitate-water system: phase diagram and state of water. Colloids Surf A 375:178–185

Bhakay A, Merwade M, Bilgili E, Dave RN (2011) Novel aspects of wet milling for the production of microsuspensions and nanosuspensions of poorly water-soluble drugs. Drug Dev Ind Pharm 37:963–976

Bibi S, Kaur R, Henriksen-Lacey M, McNeil SE, Wilkhu J, Lattmann E, Christensen D, Mohammed AR, Perrie Y (2011) Microscopy imaging of liposomes: from coverslips to environmental SEM. Int J Pharm 417:138–150

Bitterlich A, Laabs C, Busmann E, Grandeury A, Juhnke M, Bunjes H, Kwade A (2014) Challenges in nanogrinding of active pharmaceutical ingredients. Chem Eng Technol 37:840–846

Brandl M, Drechsler M, Bachmann D, Bauer K (1997) Morphology of semisolid aqueous phosphatidylcholine dispersions, a freeze fracture electron microscopy study. Chem Phys Lipids 87:65–72

Bunjes H, Drechsler M, Koch MHJ, Westesen K (2001) Incorporation of the model drug ubidecarenone into solid lipid nanoparticles. Pharm Res 18:287–293

Bunjes H, Steiniger F, Richter W (2007) Visualizing the structure of triglyceride nanoparticles in different crystal modifications. Langmuir 23:4005–4011

Burrows ND, Penn RL (2013) Cryogenic transmission electron microscopy: aqueous suspensions of nanoscale objects. Microsc Microanal 19:1542–1553

Carlton RA (2011) Pharmaceutical microscopy. Springer, New York

Cheng L, Guo S, Wu W (2009) Characterization and in vitro release of praziquantel from poly (ε-caprolactone) implants. Int J Pharm 377:112–119

Chow K, Tong HHY, Lum S, Chow AHI (2008) Engineering of pharmaceutical materials: an industrial perspective. J Pharm Sci 97:2855–2877

Corveleyn S, Remon JP (1997) Formulation and production of rapidly disintegrating tablets by lyophilisation using hydrochlorothiazide as a model drug. Int J Pharm 152:215–225

Couvreur P, Reddy LH, Mangenot S, Poupaert JH, Desmaële D, Lepêtre-Mouelhi S, Pili B, Bourgaux C, Amenitsch H, Ollivon M (2008) Discovery of new hexagonal supramolecular nanostructures formed by squalenoylation of an anticancer nucleoside analogue. Small 4:247–253

Crisp J, Dann S, Blatchford C (2011) Antisolvent crystallization of pharmaceutical excipients from aqueous solutions and the use of preferred orientation in phase identification by powder X-ray diffraction. Eur J Pharm Sci 42:568–577

Davidson MW, Fellers TJ (2003) Understanding conjugate planes and Köhler illumination. http://www.microscopyu.com/pdfs/KohlerIllumination.pdf. Accessed 30 Nov 2014

Dawidczyk CM, Russell LM, Searson PC (2014) Nanomedicines for cancer therapy: state-of-the-art and limitations to pre-clinical studies that hinder future developments. Front Chem 2:article 69

Demana PH, Davies NM, Vosgerau U, Rades T (2004) Pseudo-ternary phase diagrams of aqueous mixtures of Quil A, cholesterol and phospholipid prepared by the lipid-film hydration method. Int J Pharm 270:229–239

Devi S, Williams D (2013) Morphological and compressional mechanical properties of freeze-dried mannitol, sucrose, and trehalose cakes. J Pharm Sci 102:4246–4255

Drent P (2005) Properties and selection of objective lenses for light microscopy applications. Microsc Anal 16:5–7

Driscoll DF (2006) Lipid injectable emulsions: Pharmacopeial and safety issues. Pharm Res 23:1959–1969

Egelhaaf SU, Schurtenberger P, Müller M (2000) New controlled environment vitrification system for cryo-transmission electron microscopy: design and application to surfactant solutions. J Microsc 200:128–139

Elliot MS, Poon WCK (2001) Conventional optical microscopy of colloidal suspensions. Adv Colloid Interf Sci 92:133–194

Finke JH, Schmolke H, Klages C, Müller-Goymann CC (2013) Controlling solid lipid nanoparticle adhesion by polyelectrolyte multilayer surface modifications. Int J Pharm 449:59–71

Flegler SL, Heckman JW, Klomparens KL (1995) Scanning and transmission electron microscopy. An introduction. Oxford University Press, New York

Friedrich H, Frederik PM, deWith G, Sommerdijk NAJM (2010) Imaging of self-assembled structures: interpretation of TEM and cryo-TEM images. Angew Chem Int Ed 49:7850–7858

Gašperlin M, Kristl J, Šmid-Korbar J, Kerč J (1994) The structure elucidation of semisolid w/o emulsion systems containing silicone surfactant. Int J Pharm 107:51–56

Gaumet M, Gurny R, Delie F (2007) Fluorescent biodegradable PLGA particles with narrow size distributions: preparation by means of selective centrifugation. Int J Pharm 342:222–230

George M, Ghosh I (2013) Identifying the correlation between drug/stabilizer properties and critical quality attributes (CQAs) of nanosuspension formulation prepared by wet media milling technology. Eur J Pharm Sci 48:142–152

Ghalanbor Z, Körber M, Bodmeier R (2010) Improved lysozyme stability and release properties of poly(lactide-co-glycolide) implants prepared by hot-melt extrusion. Pharm Res 27:371–379

Ghanam D, Hassan I, Kleinebudde P (2010) Compression behaviour of κ-carrageenan pellets. Int J Pharm 390:117–127

Gilchrist SE, Letchford K, Burt HM (2012) The solid-state characterization of fusidic acid. Int J Pharm 422:245–253

Goldberg O (1980) Köhler illumination. Microscope 28:15–21

Goldstein JI, Newbury DE, Echlin P, Joy DC, Lyman CE, Lifshin E, Sawyer L, Michael JR (2003) Scanning electron microscopy and X-ray microanalysis, 3rd edn. Springer, Boston

Gong X, Moghaddam MJ, Sagnella SM, Conn CE, Danon SJ, Waddington LJ, Drummond CJ (2011) Lyotropic liquid crystalline self-assembly material behavior and nanoparticulate dispersions of a phytanyl pro-drug analogue of cepecitabine-A chemotherapy agent. ACS Appl Mater Interfaces 3:1552–1561

Grasmeijer F, Hagedoorn P, Frijlink HW, de Boer HA, Haverkamp RG (2013) Mixing time effects on the dispersion performance of adhesive mixtures for inhalation. PLoS ONE 8, e69263

Grassucci RA, Taylor DJ, Frank J (2007) Preparation of macromolecular complexes for cryo-electron microscopy. Nat Protoc 2:3239–3246

Grassucci RA, Taylor D, Frank J (2008) Visualization of macromolecular complexes using cryo-electron microscopy with FEI Tecnai transmission electron microscopes. Nat Protoc 3:330–339

Haaser M, Naelapää K, Gordon KC, Pepper M, Rantanen J, Strachan CJ, Taday PF, Zeitler JA, Rades T (2013) Evaluating the effect of coating equipment on tablet film quality using terahertz pulsed imaging. Eur J Pharm Biopharm 85:1095–1102

Harris JR (1997) Negative staining and cryoelectron microscopy. The thin film techniques. Microscopy handbooks, vol 35. BIOS Scientific Publishers in association with the Royal Microscopical Society, Oxford, UK, Herndon, VA

Harris JR (2007) Negative staining of thinly spread biological samples. In: Kuo J (ed) Electron microscopy. Methods and protocols, 2nd edn. Humana Press, Totowa, pp 107–142

Healy AM, Amaro MI, Paluch KJ, Tajber L (2014) Dry powders for oral inhalation free of lactose carrier particles. Adv Drug Deliv Rev 75:32–52

Ho R, Naderi M, Heng JYY, Williams DR, Thielmann F, Bouza P, Keith AR, Thiele G, Burnett DJ (2012) Effect of milling on particle shape and surface energy heterogeneity of needle-shaped crystals. Pharm Res 29:2806–2816

Hope MJ, Wong KF, Cullis PR (1989) Freeze-fracture of lipids and model membrane systems. J Micros Tech 13:277–287

Hoppel M, Mahrhauser D, Stallinger C, Wagner F, Wirth M, Valenta C (2014) Natural polymer-stabilized multiple water-in-oil-in-water emulsions: a novel dermal drug delivery system for 5-fluorouracil. J Pharm Pharmcol 66:658–667

Hoppentocht M, Hagedoorn P, Frijlink H, de Boer A (2014) Technological and practical challenges of dry powder inhalers and formulations. Adv Drug Deliv Rev 75:18–31

Jeong S, Park K (2008) Development of sustained release fast-disintegrating tablets using various polymer-coated ion-exchange resin complexes. Int J Pharm 353:195–204

Jeyanthi R, Thanoo B, Metha RC, DeLuca PP (1996) Effect of solvent removal technique on the matrix characteristics of polylactide/glycolide microspheres for peptide delivery. J Control Release 38:235–244

Jores K, Mehnert W, Drechsler M, Bunjes H, Johann C, Mäder K (2004) Investigations on the structure of solid lipid nanoparticles (SLN) and oil-loaded solid lipid nanoparticles by photon correlation spectroscopy, field-flow fractionation and transmission electron microscopy. J Control Release 95:217–227

Juhnke M, Märtin D, John E (2012) Generation of wear during the production of drug nanosuspensions by wet media milling. Eur J Pharm Biopharm 81:214–222

Jurasin D, Pustak A, Habus I, Smit I, Filipovic-Vincekovic N (2011) Polymorphism and mesomorphism of oligomeric surfactants: effect of the degree of oligomerization. Langmuir 27:14118–14130

Keck C (2010) Particle size analysis of nanocrystals: improved analysis method. Int J Pharm 390:3–12

Keck C, Müller RH (2008) Size analysis of submicron particles by laser diffractometry—90 % of the published measurements are false. Int J Pharm 355:150–163

Klang V, Matsko NB, Valenta C, Hofer F (2012) Electron microscopy of nanoemulsions: an essential tool for characterisation and stability assessment. Micron 43:85–103

Klang V, Valenta C, Matsko NB (2013) Electron microscopy of pharmaceutical systems. Micron 44:45–74

Kleinebudde P (1997) The crystallite-gel-model for microcrystalline cellulose in wet granulation, extrusion, and speronization. Pharm Res 14:804–809

Koning RI, Koster AJ (2009) Cryo-electron tomography in biology and medicine. Ann Anatom 191:427–445

Krauel K, Girvan L, Hook S, Rades T (2007) Characterisation of colloidal drug delivery systems from the naked eye to Cryo-FESEM. Micron 38:796–803

Kubavat HA, Shur J, Ruecroft G, Hipkiss D, Price R (2012) Investigation into the influence of primary crystallization conditions on the mechanical properties and secondary processing behaviour of fluticasone propionate for carrier based dry powder inhaler formulations. Pharm Res 29:994–1006

Kuntsche J, Westesen K, Drechsler M, Koch MHJ, Bunjes H (2004) Supercooled smectic nanoparticles: a potential novel carrier system for poorly water soluble drugs. Pharm Res 21:1834–1843

Kuntsche J, Koch M, Drechsler M, Bunjes H (2005) Crystallization behavior of supercooled smectic cholesteryl myristate nanoparticles containing phospholipids as stabilizers. Coll Surf B 44:25–35

Kuntsche J, Bunjes H, Fahr A, Pappinen S, Rönkkö S, Suhonen M, Urtti A (2008) Interaction of lipid nanoparticles with human epidermis and an organotypic cell culture model. Int J Pharm 354:180–195

Kuntsche J, Klaus K, Steiniger F (2009a) Size determinations of colloidal fat emulsions: a comparative study. J Biomed Nanotechnol 5:384–395

Kuntsche J, Koch MHJ, Fahr A, Bunjes H (2009b) Supercooled smectic nanoparticles: influence of the matrix composition and in vitro cytotoxicity. Eur J Pharm Sci 38:238–248

Kuntsche J, Freisleben I, Steiniger F, Fahr A (2010a) Temoporfin-loaded liposomes: physico-chemical characterization. Eur J Pharm Sci 40:305–315

Kuntsche J, Koch MH, Steiniger F, Bunjes H (2010b) Influence of stabilizer systems on the properties and phase behavior of supercooled smectic nanoparticles. J Coll Interf Sci 350:229–239

Kuntsche J, Horst JC, Bunjes H (2011) Cryogenic transmission electron microscopy (cryo-TEM) for studying the morphology of colloidal drug delivery systems. Int J Pharm 417:120–137

Lauf U, Fahr A, Westesen K, Ulrich AS (2004) Novel lipid nanotubes in dispersions of DMPC. ChemPhysChem 5:1246–1249

Lee WL, Seh YC, Widjaja E, Chong HC, Tan NS, Joachim Loo SC (2012) Fabrication and drug release study of double-layered microparticles of various sizes. J Pharm Sci 101:2787–2797

Li X, Hirsh DJ, Cabral-Lilly DZA, Gruner SM, Janoff AS, Perkins WR (1998) Doxorubicin physical state in solution and inside liposomes loaded via a pH gradient. Biochim Biophys Acta 1415:23–40

Lindfors L, Skantze P, Skantze U, Westergren J, Olsson U (2007) Amorphous drug nanosuspensions. 3. Particle dissolution and crystal growth. Langmuir 23:9866–9874

Littringer EM, Noisternig MF, Mescher A, Schroettner H, Walzel P, Griesser UJ, Urbanetz NA (2013) The morphology and various densities of spray dried mannitol. Powder Technol 246:193–200

Madsen HB, Arboe-Andersen HM, Rozlosnik N, Madsen F, Ifversen P, Kasimova MR, Nielsen HM (2010) Investigation of the interaction between modified ISCOMs and stratum corneum lipid model systems. Biochim Biophys Acta 1798:1779–1789

Mercuri A, Belton PS, Royall PG, Barker SA (2012) Identification and molecular interpretation of the effects of drug incorporation on the self–emulsification process using spectroscopic, micropolarimetric and microscopic measurements. Mol Pharmaceutics 9:2658–2668

Meyer H, Richter W (2001) Freeze-fracture studies on lipids and membranes. Micron 32:615–644

Muhsin Ö, Höglund S, Gelderblom HR, Morein B (1989) Quarternary structure of the immunostimulating complex (Iscom). J Ultrastruc Mol Struc Res 102:240–248

Müller-Goymann CC (1984) Liquid crystals in emulsions, creams, and gels containing ethoxylated sterols as surfactant. Pharm Res 4:154–158

Munk T, Baldursdottir S, Hietala S, Rades T, Kapp S, Nuopponen M, Kalliomäki K, Tenhu H, Rantanen J (2012) Crystal morphology modification by the addition of tailor–made stereocontrolled poly(N-isopropyl acrylamide). Mol Pharmaceutics 9:1932–1941

Nagy ZK, Balogh A, Vajna B, Farkas A, Patyi G, Kramarics Á, Marosi G (2012) Comparison of electrospun and extruded Soluplus®-based solid dosage forms of improved dissolution. J Pharm Sci 101:322–332

Narayan P, Hancock BC (2003) The relationship between the particle properties, mechanical behavior, and surface roughness of some pharmaceutical excipient compacts. Mat Sci Eng A 355:24–36

Nichols G, Frampton CS (1998) Physicochemical characterization of the orthorhombic polymorph of paracetamol crystallized from solution. J Pharm Sci 87:684–693

Nonomura Y, Nakayama K, Aoki Y, Fujimori A (2009) Phase behavior of bile acid/lipid/water systems containing model dietary lipids. J Colloid Interf Sci 339:222–229

Oheim M, Micheal DJ, Geisbauer M, Madsen D, Chow RH (2006) Principles of two-photon excitation fluorescence microscopy and other nonlinear imaging approaches. Adv Drug Del Rev 58:788–808

Oldenbourg R (1996) A new view on polarization microscopy. Nature 381:811–812

Otte A, Carvajal MT (2011) Assessment of milling-induced disorder of two pharmaceutical compounds. J Pharm Sci 100:1793–1804

Pajander J, Haugshøj KB, Bjørneboe K, Wahlberg P, Rantanen J (2013) Foreign matter identification from solid dosage forms. J Pharm Biopharm Anal 80:116–125

Paspaleeva-Kühn V, Nürnberg E (1992) Participation of macrogolstearate 400 lamellar phases in hydrophilic creams and vesicles. Pharm Res 9:1336–1340

Pingali KC, Mendez R (2014) Nanosmearing due to process shear—influence on powder and tablet properties. Adv Powder Technol 25:952–959

Piston DW (1998) Choosing objective lenses: the importance of numerical aperture and magnification in digital optical microscopy. Bio Bull 195:1–4

Pitchayajittipong C, Price R, Shur J, Kaerger JS, Edge S (2010) Characterisation and functionality of inhalation anhydrous lactose. Int J Pharm 390:134–141

Pluta M (1969) A phase-contrast device with positive and negative image contrast. J Microsc 89:205–216

Prehm M, Enders C, Anzahaee MY, Glettner B, Baumeister U, Tschierke C (2008) Distinct columnar and lamellar liquid crystalline phases formed by new bolaamphiphiles with linear and branched lateral hydrocarbon chains. Chem Eur J 14:6352–6368

Rades T, Müller-Goymann CC (1997) Electron and light microscopical investigation of defect structures in mesophases of pharmaceutical substances. Colloid Polym Sci 275:1169–1178

Raijada D, Genina N, Fors D, Wisaeus E, Peltonen J, Rantanen J, Sandler N (2013) A step toward development of printable dosage forms for poorly soluble drugs. J Pharm Sci 102:3694–3704

Rank A, Hauschild S, Förster S, Schubert R (2009) Preparation of monodisperse block copolymer vesicles via a thermotropic cylinder – vesicle transition. Langmuir 25:1337–1344

Rasenack N, Müller BW (2002) Dissolution rate enhancement by in situ micronization of poorly water-soluble drugs. Pharm Res 19:1894–1900

Rizwan S, Dong Y, Boyd B, Rades T, Hook S (2007) Characterisation of bicontinuous cubic liquid crystalline systems of phytantriol and water using cryo field emission scanning electron microscopy (cryo FESEM). Micron 38:478–485

Rosenblatt KM, Bunjes H (2009) Poly(vinyl alcohol) as emulsifier stabilizes solid triglyceride drug carrier nanoparticles in the α-modification. Mol Pharmaceutics 6:105–120

Rowe RC, Sheskey PJ, Quinn ME (2009) Handbook of pharmaceutical excipients, 6th edn. Pharmaceutical Press, London

Savic S, Vuleta G, Daniels R, Müller-Goymann CC (2005) Colloidal microstructure of binary systems and model creams stabilized with an alkylpolyglucoside non-ionic emulsifier. Colloid Polym Sci 283:439–451

Schmidt PC (2002) Secondary electron microscopy in pharmaceutical technology. In: Swarbrick J, Boylan JC (eds) Encyclopedia of pharmaceutical technology, vol 3, 2nd edn. Marcel Dekker, New York, pp 2401–2435

Schütze W, Müller-Goymann CC (1992) Mutual interactions between nonionic surfactants and gelatin—investigations in cubic liquid crystalline systems and micellar systems. Colloid Polym Sci 269:85–90

Scoutaris N, Vithani K, Slipper I, Chowdhry B, Douroumis D (2014) SEM/EDX and confocal Raman microscopy as complementary tools for the characterization of pharmaceutical tablets. Int J Pharm 470:88–98

Seefeldt K, Miller J, Alvarez-Nunez F, Nodriguez-Hornedo N (2007) Crystallization pathways and kinetics of carbamazepine-nicotinamide cocrystals form the amorphous state by *in situ* thermomicroscopy, spectroscopy and calorimetry studies. J Pharm Sci 96:1147–1158

Severs NJ (2007) Freeze-fracture electron microscopy. Nat Protoc 2:547–576

Siekmann B, Westesen K (1995) Preparation and physicochemical characterization of aqueous dispersions of coenzyme Q10 nanoparticles. Pharm Res 12:201–208

Spring KR, Keller HE, Davidson MW (2014) Microscope objectives introduction. http://www.olympusmicro.com/primer/anatomy/objectives.html. Accessed 30 Nov 2014

Sternberg B, Sorgi FL, Huang L (1994) New structures in complex formation between DNA and cationic liposomes visualized by freeze-fracture electron microscopy. FEBS Lett 356:361–366

Tian F, Baldursdottir S, Rantanen J (2009) Effects of polymer additives on the crystallization of hydrates: a molecular-level modulation. Mol Pharmaceutics 6:202–2010

Unruh T, Westesen K, Bösecke P, Lindner P, Koch MHJ (2002) Self-assembly of triglyceride nanocrystals in suspension. Langmuir 18:1796–1800

van Eerdenbrugh B, Froyen L, van Humbeeck J, Martens JA, Augustijns P, van den Mooter G (2008) Alternative matrix formers for nanosuspension solidification: dissolution performance and X-ray microanalysis as an evaluation tool for powder dispersion. Eur J Pharm Sci 35:344–353

Vehring R (2008) Pharmaceutical particle engineering via spray drying. Pharm Res 25:999–1022

Velluto D, Demurtas D, Hubbell JA (2008) PEG-b-PPS diblock copolymer aggregates for hydrophobic drug solubilization and release: cyclosporin A as an example. Mol Pharmaceutics 5:632–642

Vielreicher M, Schürmann S, Detsch R, Schmidt MA, Buttereit A, Boccaccini A, Friedrich O (2013) Taking a deep look: modern microscopy technologies to optimize the design and functionality of biocompatible scaffolds for tissue engineering in regenerative medicine. J R Soc Interface 10:0263

Villalobos-Hernández J, Müller-Goymann C (2005) Novel nanoparticulate carrier system based on carnauba wax and decyl oleate for the dispersion of inorganic sunscreens in aqueous media. Eur J Pharm Biopharm 60:113–122

Weaver R (2003) Rediscovering polarized light microscopy. American Lab 35:55–61

Westesen K, Wehler T (1992) Physicochemical characterization of a model intravenous oil-in-water emulsion. J Pharm Sci 81:777–786

White NS, Errington RJ (2005) Fluorescence techniques for drug delivery research: theory and practice. Adv Drug Del Rev 57:17–42

Williams DB, Carter CB (2009) Transmission electron microscopy. A textbook for materials science, 2nd edn. Springer, New York

Witt C, Kissel T (2001) Morphological characterization of microspheres, films and implants prepared from poly(lactide-co-glycolide) and ABA triblock copolymers: is the erosion controlled by degradation, swelling or diffusion? Eur J Pharm Biopharm 51:171–181

Wu JX, Xia D, van den Berg F, Amigo JM, Rades T, Yang M, Rantanen J (2012) A novel image analysis methodology for online monitoring of nucleation and crystal growth during solid state phase transformations. Int J Pharm 433:60–70